Robotic Non-destructive Test of Concrete Structures with GPR, Impact Echo and 3D Vision

Sajjad Sayyar Roudari, Theophilus Okore-Hanson, Sameer Hamoush, Younho Seong, Sun Yi, Taylor Szeto, Jean Plummer

Robotic Non-destructive Test of Concrete Structures with GPR, Impact Echo and 3D Vision – 19540

Sajjad Sayyar Roudsari *, Theophilus Okore-Hanson *, Sameer Hamoush *, Younho Seong *, Sun Yi *, Taylor Szeto *, Jean Plummer **

* North Carolina A&T State University (NCAT), Greensboro, NC, 27411

** Savannah River National Laboratory (SRNL), Aiken, SC, 29808

ABSTRACT

Structural members come across with various internal defects that cannot be evaluated visually. Instead, hand-held nondestructive sensors are used to detect such defects. In many situations, the hand-held NDT is not possible in high-risk structures because of limited access or safety issues. Therefore, Robotic NDT plays major role in assessing such structures. Robot Operating Systems (ROS) is a powerful open source tool, which is used to program and control robots and other devices enabling one to use sensors, devices and new functionalities such as autonomous navigation, visual perception. For the research presented, ROS is used to program the Sawyer robot arm manufactured by Rethink Robotics. The control system for the robot ensures the ability to adapt to different weights of integrated measuring devices and measured force applied against the wall with a wheeled measuring device while making a remote sweep. Twelve reinforced concrete (RC) beams built with characterized defects are evaluated with the robotic arm integrated with the measuring devices. The RC beams are characterized by voids, corrosion and debonding problems of rebars. The Impact Echo and Ground Penetrating Radar (GPR) devices attached to the robot arm are used to measure the material properties of the concrete beams. The robot arm ensures consistency and uniformity of measurement even in obscure locations. Infrared cameras are used to obtain 3D images of the surfaces of the concrete structures. Roughness is analyzed using computer vision techniques prior to the use of other sensors that are in touch with the surfaces. The computer vision is also used to handle the images collected from GPR sensor. Hand-held NDE is also performed to verify the results obtained by robotic examination.

INTRODUCTION

Nondestructive evaluation (NDE) is one of the most common methods to inspect the structural elements. This technique is useful to find out the deterioration, cracks, inside and outside defects on structural members. As for concrete material, different equipment has been using depending capability to figure the defects out. Generally, nondestructive equipment uses either the vibration as a part of signal processing, also the laser technique has been employing to compute the frequency, velocity, wavelength and so on *(Singh et al. 1986, Santos et al. ERD for NDT, Ahn et al. 2017)*. In this regard, three important waves can be carried out to investigate the concrete material properties and qualities which are P-Wave, S-Wave and Rayleigh Waves *(Hung et al 2017).* There are so many causes done to evaluate the reinforced concrete (RC) structure using nondestructive device as Ground Penetrating Radar (GPR) and Impact Echo (IE).

Using these-equipment helped scientists and researchers distinguish the defects inside of RC structures *(Dinh et al. 2017 and 2018*). On the other hand, the hand-held NDE is not always practical because structures may be in un-safe environments or inspecting is hard to be done by human. Therefore, the use robots can contribute to avoid inconvenience problems *(Morozov et al. 2018, Manh La et al. 2017).* The heart of the mattered is that the robotic NDE has been done for inspecting bridge deck to evaluate any kind of deficiency of bridges. As it is clear, the bridges are one of the critical infrastructures over the world *(Asmari et al. 2017, Pizarro et al. 2010).*

But, on the other side, the evaluation of other structural elements is critical, as a case in point, tunnels, dams, nuclear energy structures and just to name a few. So, the robotic side needs to develop, in advance.

In this paper, different reinforced concrete (RC) beam have been built in the North Carolina A&T State University using robotic NDE laboratory. The RC beams have been made to have various defect on purpose. The hand-held and robotic Impact Echo, GPR and 3D vision Camera are used to evaluate and analyze the results by comparing.

EXPERIMENTAL TESTS (METHODS, DISCUSSION, CONCLUSIONS)

In this paper, twelve reinforced concrete beams are built so that they are subjected to have different type of internal and external defects. The defects inside the RC beams include void, corrosion, debonding and honeycombing. As a matter of fact, the RC beams are divided into four different groups. In general, honeycombing is considered as an extra deficiency on RC beams. The RC beams are shown in **Fig1**, and the group division and names are shown in the **Table1**. The RC beams have the dimension of $96 \times 16 \times 8$ inches ($2400 \times 400 \times 200\, mm$) as length, height and width. Only #4 (12.7 mm diameter) bars have been employed in the bottom side of beam as tension area. This RC beam does not need to have stirrups since shear force is small and ignorable. The concrete compressive strength is assigned as 4000 Psi (27.5 MPa). Table2 shows the geometry and location of void inside of concrete. The corroded bars have been made naturally by plunging in the water. Debonding issue is also made by lubricating bars to be completely un-touch with concrete core.

Figure 1. RC Beams uses for the NDE Research

Table 1. Group of the RC Beams used for experiments

Group Name	A	B	C	D	Extra Defect
Type	Control	Void	Corrosion	Debonding	Honeycombing

Table 2. Geometry - Properties and Void location of RC Beam

Beam	**Length, inch (mm)**	**Depth, inch (mm)**	**Width, inch (mm)**
	96 (2400)	16 (40)	8 (20)
Bar	**Number of Bar**	**Longitudinal Bar Diameter (mm)**	**Transvers Bar Diameter**
	4	#4 (12.7)	Not Use

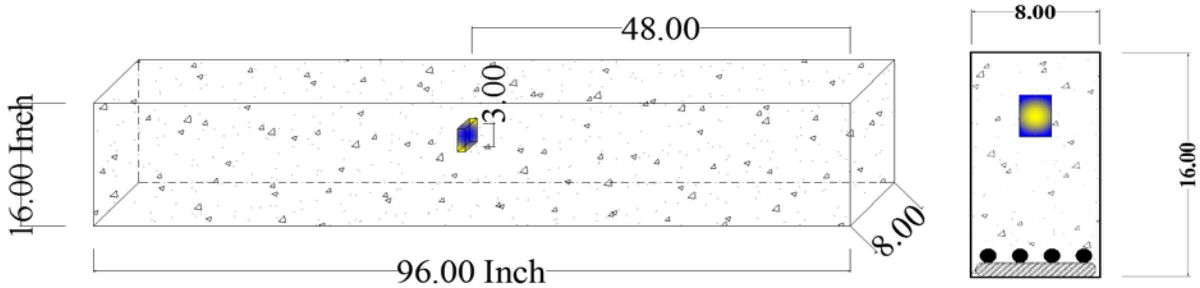

Investigation Items

In this research, Sawyer robot is used to carry NDT sensor and camera. This robot can be controlled by Intera Studio, which utilizes high resolution sensors in each joint. The sensors measure the force and adjust in a required situation. The manipulation of force control has two factors as impedance like classical and dynamic control and hybrid control. **Figure2** presents the Sawyer Robot features. In this section, three different sensors have been employed as IE (Impact Echo), GPR (Ground Penetrating Radar) and Intel RealSense D435 Depth Camera. The first sensor uses frequency to obtain the module of elasticity and shear modulus are some of its results. The penultimate is a kind of laser scanner to find out the inside defects giving the visual image of inside deterioration. The RealSense D435 Camera can be as used to find out the honeycombing issue. In the research, four RC beams are tested by hand-held NDE equipment and then the robot is utilized to carry the equipment out. **Figures 3**,**4** and **5** display robotic evaluation of GPR, IE and also D435 Camera, in order.

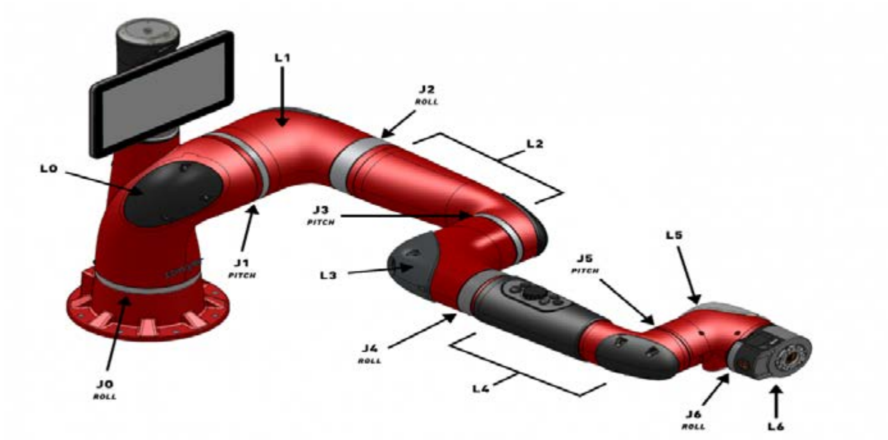

Figure 2. Sawyer Robot Features

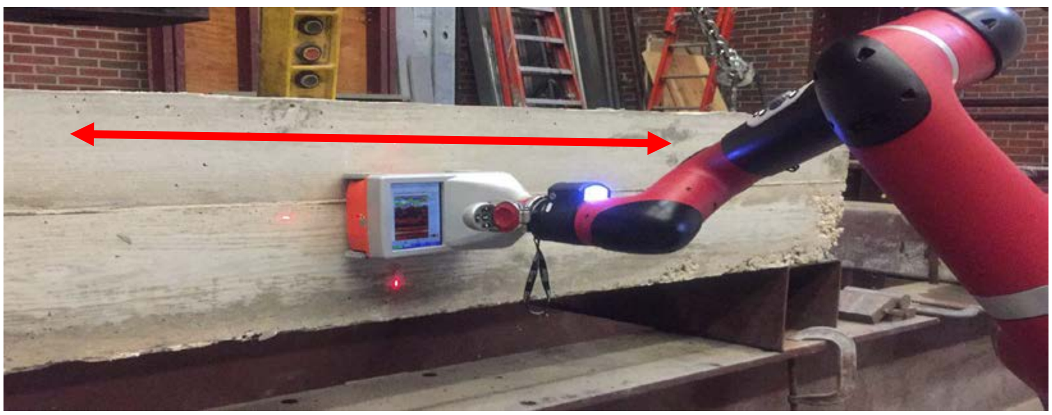

Figure 3. Robotic GPR

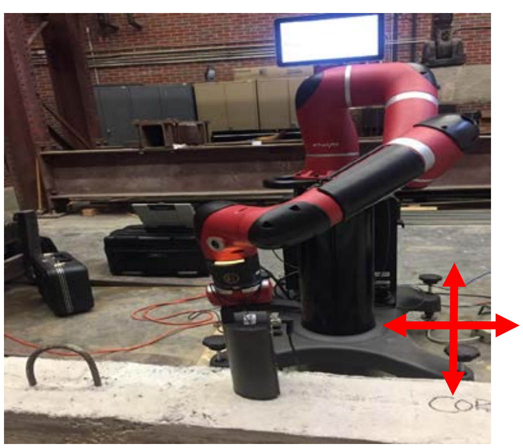

Figure 4. Robotic Impact Echo (IE)

Figure 5. The RealSense D435 Depth Camera

Results and Discussion

After doing both robotic and hand-held IE, GPR and D435 Camera, the results of each specimen are evaluated. In effect, the IE test gives the module of elasticity based on the quality of frequency, wavelength and velocity and according to ACI standard *(ACI Committee 318)*, the compressive strength of concrete can be computed using.

$$E_c = 33\, W_c^{1.5} \sqrt{f_c}$$

(1)

For computing, the MATLAB plot toolbox is employed to calculate the compressive strength of concrete based on module of elasticity. The result of compressive strength is shown in **Fig6**. As it can be seen in this figure, the control sample (A) has much more compressive strength value (unit: Psi). The comparison among defected specimens and un-defected ones illustrate the effects of void, corrosion and debonding in RC beams. In other word, if the hand-held IE takes into consideration, it can be declared that, the compressive strength of RC beam with inside void (B) has about 88.4% reduction compared to control sample (A). Granted the corrosion (Group C) and debonding (group D) have almost the same compressive strength but, contrasting them to control sample can be demonstrate that they have about 72.9% and 73.5% reduction of compressive strength, respectively.

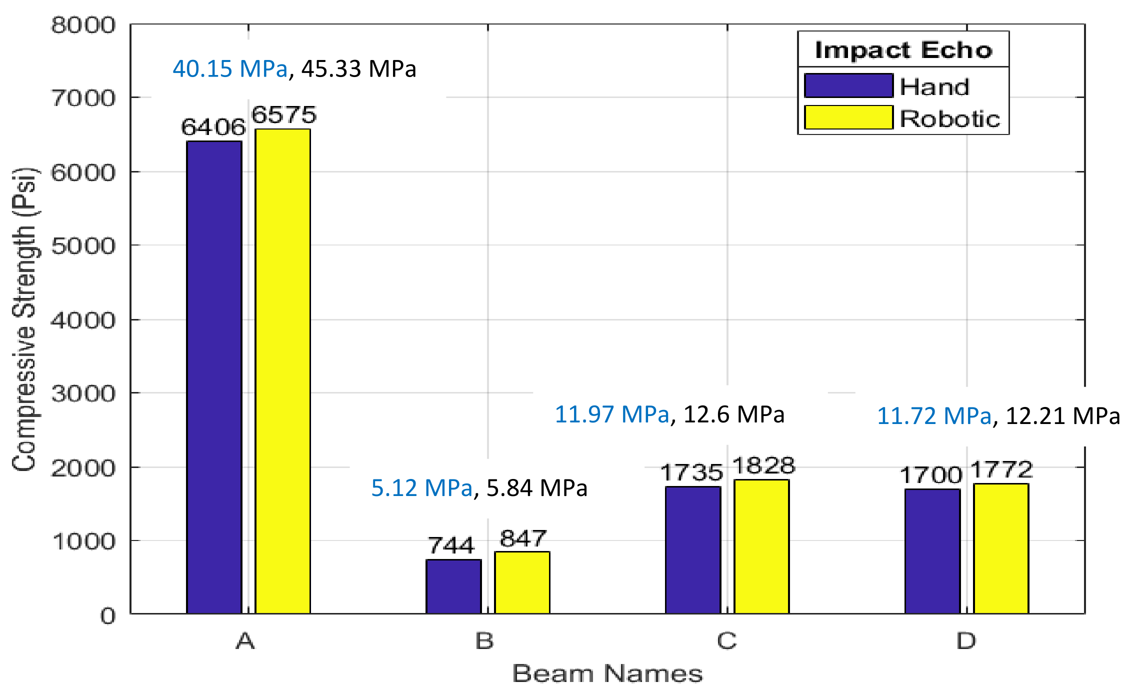

Figure 6. Compressive Strength - Hand-Held and Robotic Impact Echo (Psi)

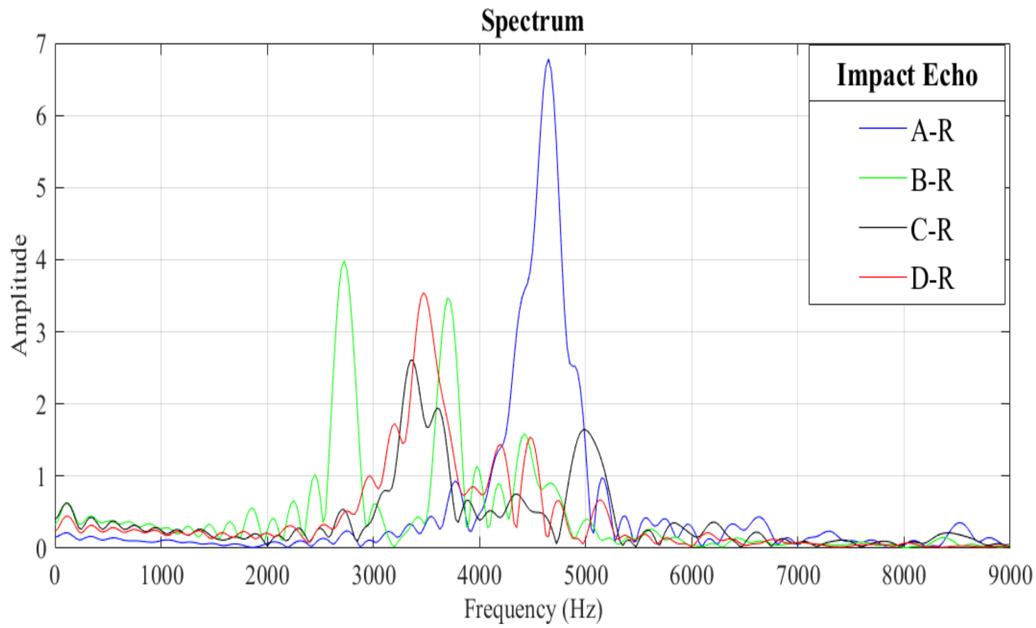

Figure 7. Frequency Amplitude of Robotic Impact Echo

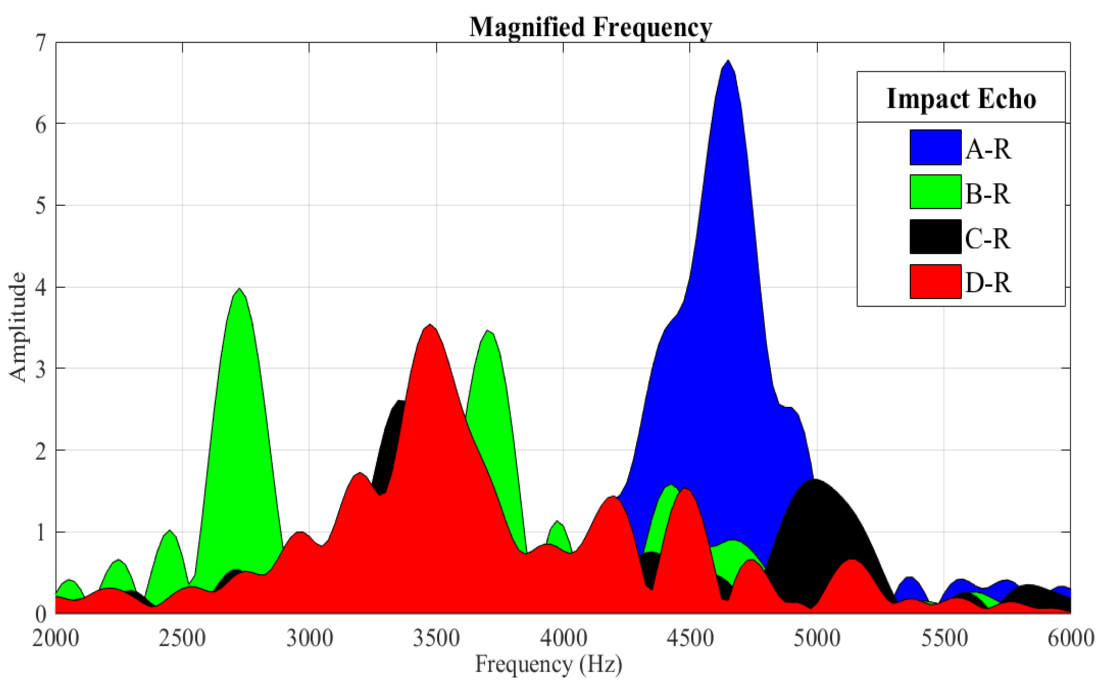

Figure 8. Magnified Area Plot of Frequency-Amplitude of Impact Echo

The difference between robotic and hand-held uses compared. The robotic IE about 2.65% more value in compressive strength than hand-held IE. Also, the difference of robotic IE for the groups B, C and D is about 13.9, 5.35 and 4.25 percent, in order meaning that robotic and hand-held tests have very good agreement. In **Figs 7** and **8**, the frequency distribution of robotic IE is shown. In **Fig 7**, the frequency of the control sample is not fluctuated, and it only has one smooth peak indicating the concrete has not any inside deterioration and defect. But the void (B), corrosion (C) and debonding (D) specimens have multiple fluctuations meaning that the reflected frequency collides some defects which can cause different amplitude.

In this case, **Fig 8** shows a magnified image of **Fig 7** to can approve that the difference of the frequency distribution based on each defect. The specimens show that there are more than at least two summits beside each other. When other summits amplitude value is more than 20 percent of the biggest peak, it can be declared that there are some deficiencies inside of concrete. In this regard, the pattern of defects is difference as a case in point, the void specimen (B-R) has two big peaks of which the wavelength is long demonstrating that the reflected frequency has lower velocity. On the other hand, the corrosion (C-R) result has its own pattern as multiple peaks by having very long wavelength. Compares to deboning sample (D-R), the wave length is shorter than corrosion sample, but the amplitude is larger. The frequency distribution has a range up to 15000 Hz and after 9000 Hz, it displays trivial amount of amplitude. On the other side, the hand-held and robotic GRP is also used for GPR evaluation.

Furthermore, **Figs 9** to **12** display the comparison on hand-held and robotic GPR. **Figure.9**, show there is not any defect inside of the RC beam and the white color which can be seen at the end of rebars (bottom) presents the pole as steel plate for making the concrete cover. In addition, in **Fig 10**, the comparison of both is shown for the void specimen (B). this figure shows there are some defects inside of RC beam indicating that the void which is created my foam is located almost at the center of the beam. The top right and left images show the hoops were embedded to lift the beam. The damaged area of the hoops also presents that the delamination happened. Moreover, there are two white spots under the ends of rebars observed. These are the curve shape plate which were employed to make a constant cover between bars and concrete surface. **Figures 11** and **12** also present the GPR evaluation for corrosion and debonding samples. These defects affect the color of bars such a way that the highlighted spots are demonstrating how the corroded or de-bonded bars can be different in comparison to other spots.

Hand-Held GPR

AH

Robotic – GPR

AR

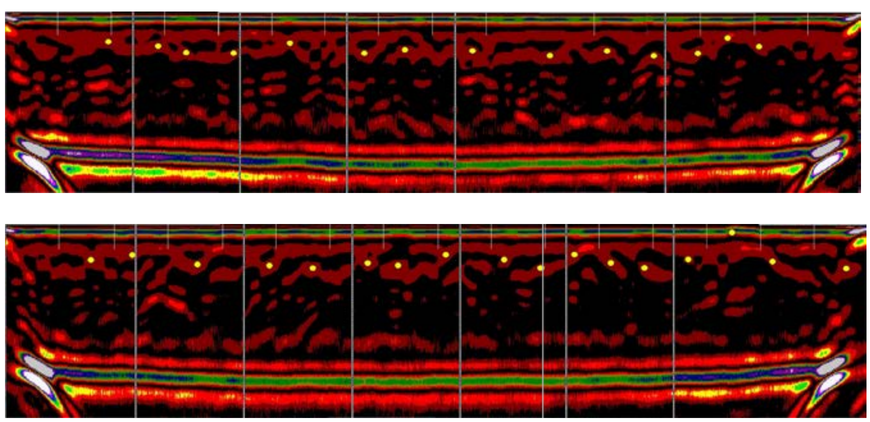

Figure 9. Robotic Compared with Hand-Hel GPR - Control Specimen

Hand-Held GPR

BH

Robotic – GPR

BR

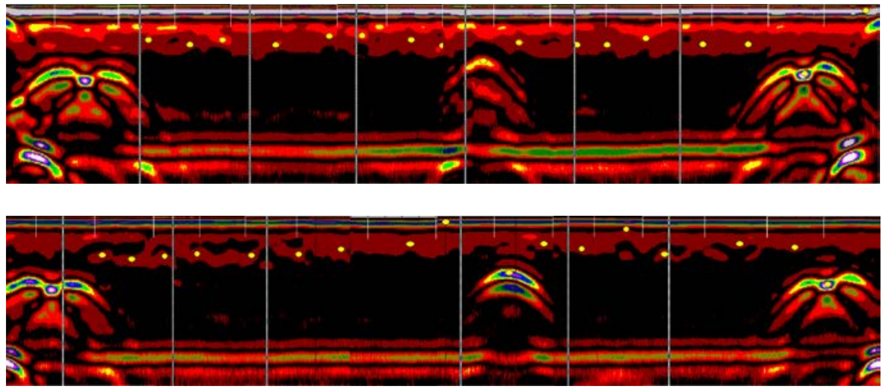

Figure 10. Robotic Compared with Hand-Hel GPR - Void Specimen

Hand-Held GPR

CH

Robotic – GPR

CR

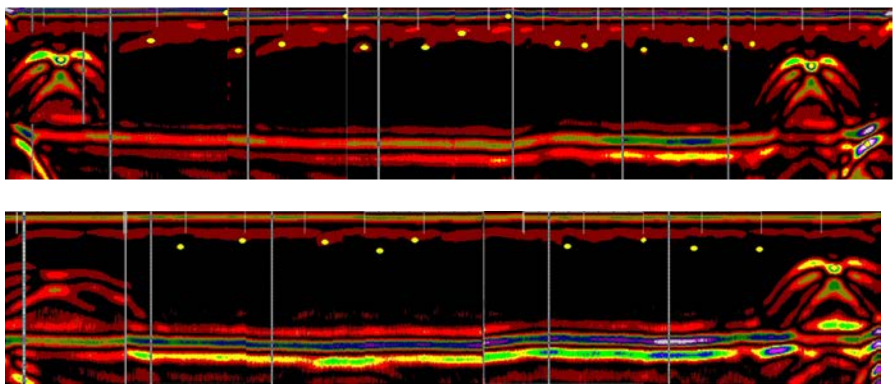

Figure 11. Robotic Compared with Hand-Hel GPR - Corrosion Specimen.

Hand-Held GPR

DH

Robotic – GPR

DR

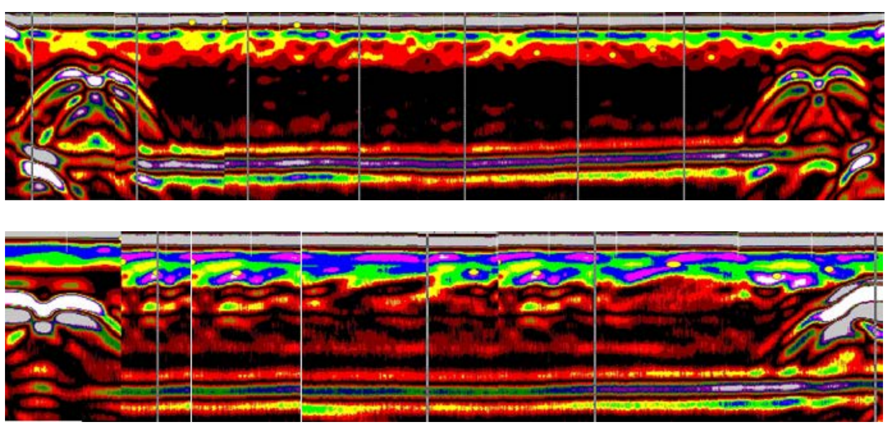

Figure 12. Robotic Compared with Hand-Hel GPR - Debonding Specimen.

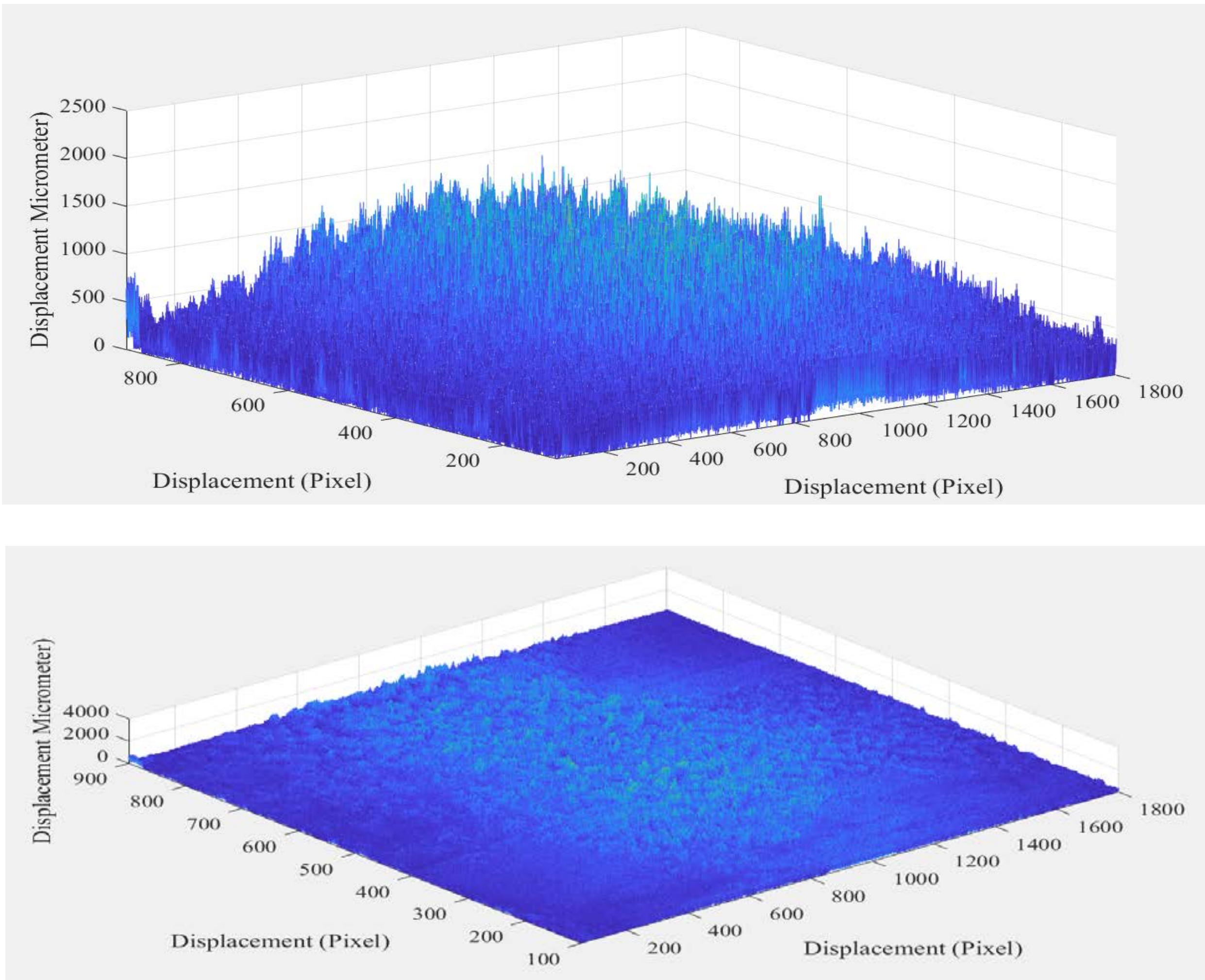

Figure 13. D435 Real Sense Camera of RC beam

In **Fig.13**, the real sense camera result is shown. The Image Acquisition application is used to record the results by MATLAB toolbox. Moreover, the meshing plot technique is used to visualize the image. The noise issue is solved by limiting the out layers area to display the real pixel of data for RC beam's surface. This figure shows the honeycombing surface of RC beam has different pixel of smooth surfaces. Specially, in the bottom image of **Fig.**13, the depth of honeycombing area is clear by looking at Z direction. Comparing these criteria helps to distinguish the depth of roughness as well. The real comparison of real sense camera scanning versus the experimental RC beam is shown in **Fig.14** so that these two images have very good agreement.

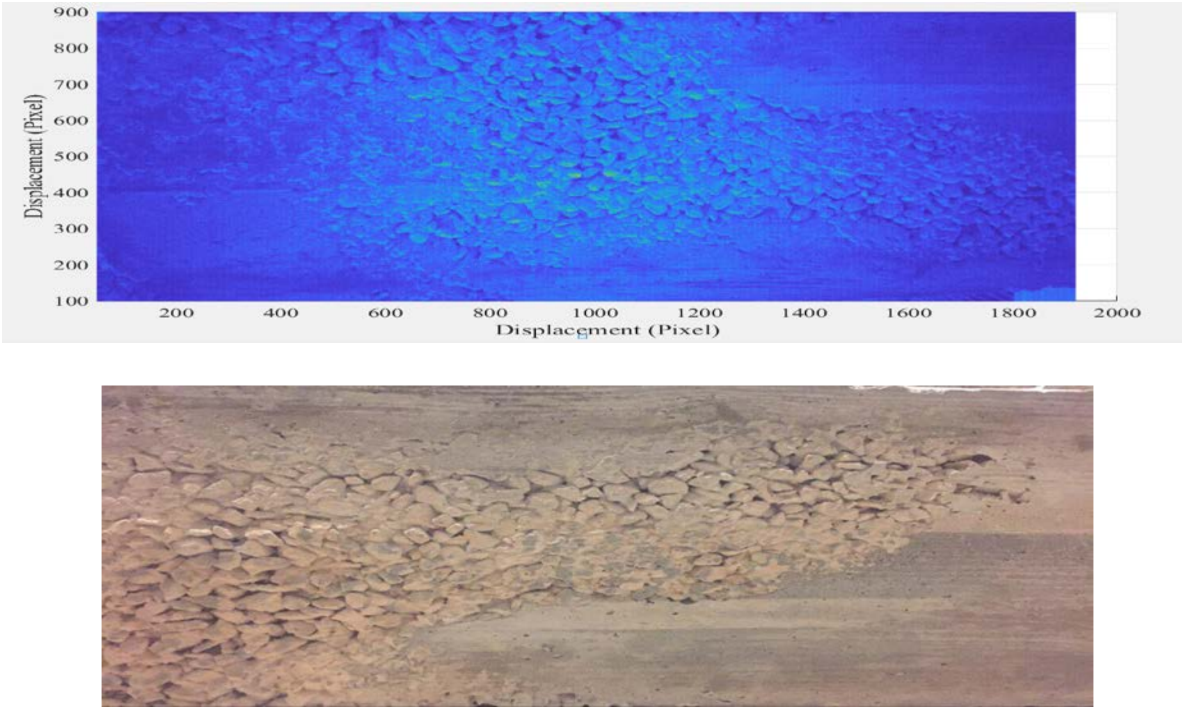

Figure 14. Comparison of Real Image of Honeycombing Area versus Scanned by Real Sense Camera

Conclusion

This research has evaluated the effect of different defects inside and on the surface of RC beams. The results are as follows;

- The robotic IE and GPR have very good agreement with hand-held ones.
- The void defect causes much more reduction of compressive strength compared to control sample, while the corrosion and debonding have almost the same reduction of compressive strength.
- The one summit indicates the good quality of concrete, but fluctuated peaks show there are some defects inside of RC beam.
- The real sense camera can visualize the honeycombing area of concrete surface and the depth of the roughness.

REFERENCES

ACI Committee 318., "Building Code Requirements for Structural Concrete (ACI318M-11) and Commentary," American Concrete Institute, Farmington Hills, Mich., USA, 2011

Ali Asmari., Andrew Marrero., and Ebi Maher., "Autonomous Navigation and Geotagging for Concrete Bridge Deck Inspections with the RABIT Robotic Platform", Conference: American Society of Nondestructive Testing 2017

C.-C. Hung., Wei-Ting Lin., K.-C. Pai., "Concrete compressive strength identification by impact-echo method" July 2017 Computers and Concrete 20(1):49-56, DOI: 10.12989/cac.2017.20.1.049

Castillo-Pizarro, P., T.V. Arredondo, and M. Torres-Torriti. Introductory survey to open-source mobile robot simulation software. in Robotics Symposium and Intelligent Robotic Meeting (LARS), 2010 Latin American. 2010. IEEE

Eunjong Ahn., Hyunjun Kim., Sung-Han Sim., Sung Woo Shin., Myoungsu Shin., "Principles and Applications of Ultrasonic-Based Nondestructive Methods for Self-Healing in Cementitious Materials", Materials 2017, 10, 278; doi:10.3390/ma10030278

G.P. Singh, S. Udpa,." The role of digital signal processing in NDT", June 1986 NDT International 19(3):125-132.

Hung Manh La., Nenad Gucunski., Kristin J. Dana., Kristin J. Dana., Seong-Hoon Kee., "Development of An Autonomous Bridge Deck Inspection Robotic System", April 2017 Journal of Field Robotics, DOI: 10.1002/rob.21725.

Kien Dinh., Nenad Gucunski., Jinyoung Kim., Trung Huy Duong.," Method for attenuation assessment of GPR data from concrete bridge decks" August 2017 , NDT & E International 92, DOI: 10.1016/j.ndteint.2017.07.016

Kien Dinh., Nenad Gucunski., Trung Huy Duong., " An algorithm for automatic localization and detection of rebars from GPR data of concrete bridge decks" February 2018 Automation in Construction 89:292–298, DOI: 10.1016/j.autcon.2018.02.017

M. Morozov., S.G. Pierce, C.N. MacLeod, C. Mineo, R. Summan., "Off-line scan path planning for robotic NDT.", Measurement 122 (2018) 284–290., Doi.org/10.1016/j.measurement.2018.02.020.

Serge Dos Santos, Zdenek Prevorovsky, Christophe Mattei, Valeriy Vengrinovich, Giuseppe Nardoni and Julian Wright, "European Research Day (ERD) Academia NDT International Workshop, Nonlinear Signal Processing for NDT 4.0.

ACKNOWLEDGEMENTS

The study of this research is financially supported by Savannah River National Laboratory.